Available online at www.sciencedirect.com
ScienceDirect
Journal of Computational Physics 226 (2007) 1219–1233
JOURNAL OF COMPUTATIONAL PHYSICS
www.elsevier.com/locate/jcp

Numerical simulation of nonlinear dynamical systems driven by commutative noise

F. Carbonell [a,*], R.J. Biscay [a], J.C. Jimenez [a], H. de la Cruz [b,c]

[a] *Institute for Cybernetics, Mathematics and Physics, Department of Interdisciplinary Mathematics, Havana, Cuba*
[b] *Granma University, Department of Mathematics and Computation, Bayamo MN, Cuba*
[c] *University for Informatics Sciences, Havana, Cuba*

Received 6 October 2006; received in revised form 3 May 2007; accepted 21 May 2007
Available online 8 June 2007

Abstract

The local linearization (LL) approach has become an effective technique for the numerical integration of ordinary, random and stochastic differential equations. One of the reasons for this success is that the LL method achieves a convenient trade-off between numerical stability and computational cost. Besides, the LL method reproduces well the dynamics of nonlinear equations for which other classical methods fail. However, in the stochastic case, most of the reported works has been focused in Stochastic Differential Equations (SDE) driven by additive noise. This limits the applicability of the LL method since there is a number of interesting dynamics observed in equations with multiplicative noise. On the other hand, recent results show that commutative noise SDEs can be transformed into a random differential equation (RDE) by means of a random diffeomorfism (conjugacy). This paper takes advantages of such conjugacy property and the LL approach for defining a LL scheme for SDEs driven by commutative noise. The performance of the proposed method is illustrated by means of numerical simulations.

MSC: 60H10; 60H25; 60H35; 65C30

Keywords: Local linearization; Stochastic differential equations; Commutative noise; Conjugacy; Random differential equations; Numerical integrators

1. Introduction

In several physical, chemical and biological phenomena, noise plays a significant role. This is the case, for example, in turbulent diffusion, genetic regulation, chemical kinetic, biological waste treatment, polymer dynamics and large scale integrated (VLSI) circuit design. When the evolution of such noisy phenomena has to be studied, the mathematical modeling of such situations is not well matched by deterministic differen-

* Corresponding author.
E-mail address: felix@icmf.inf.cu (F. Carbonell).

0021-9991/$ - see front matter
doi:10.1016/j.jcp.2007.05.024

tial equations. In these cases, stochastic differential equations (SDEs) are more suitable when a more realistic modeling needs to be considered. Since, unfortunately, analytic solutions of the equations are rarely available, in recent years much attention has been paid to design numerical methods for approximating their solutions.

A variety of examples of SDEs used for modeling nonlinear physical systems are defined by quite complicated drift components but relatively simple diffusion terms [1]. For instance, equations driven either by a single Wiener process or by commutative noise (understood as commutativity of the diffusion vector fields in the sense of Lie algebras). In these situations the simplicity in the diffusion terms of the equations has allowed the development of analytical methods for the better understanding of their dynamics. Perhaps the most interesting results are those dealing with the extant conjugacy (diffeomorfism that performs an stationary random coordinate change) between random differential equations (RDE) and commutative noise SDEs [1–3]. This idea goes back to the Doss's representation of diffusions [4] and rests upon the decomposition of the flow by the Itô Ventzell formula [5]. The main advantage of such approach comes from the fact that objects of interest in random dynamics (i.e. random fixed points, random attractors, random bifurcations, etc.) are harder to describe in the framework of stochastic calculus than in the framework of classical deterministic calculus. For instance, the conjugacy property has been already used for establishing the existence of global attractors in SDEs [1] and for stating a Hartman–Grobman theorem for this kind of equations [3].

The aim of this paper is to take advantage of the extant conjugacy property between random and stochastic equations in order to construct a numerical method for the integration of SDEs driven by commutative noise. This idea of using an auxiliary RDE for solving a SDE is not new in the context of numerical methods. In fact, it is called the ODE approach for solving SDEs and it has been well-studied in the literature [6–8]. However, this paper is the first attempt of using the conjugacy property for defining a numerical method for SDEs. In this way, our approach opens new opportunities for the comparison of the long-time behavior of SDEs and their numerical approximations. Indeed, it is possible to study the numerical dynamics of a SDE by just analyzing its conjugate RDE, which is possible by simple pathwise classical (deterministic) arguments.

A key stone in the derivation of the numerical integrator introduced in this paper is the local linearization (LL) technique, which directly allows the use of the analytical expression for the conjugacy between pure noise linear SDEs and RDEs. This linearization approach has been previously used to derive a class of stable and efficient numerical methods for ODEs, RDEs and SDEs (see for instance [9–12] and references therein). The basic components of the LL approach are the piecewise linear approximation (by the first-order Taylor expansion) of the vector fields and the numerical integration (often exact) of the resulting linear equation. In the case of SDEs, the LL approach has been restricted either to the class of equations with additive noise terms or scalar equations with multiplicative noise. Therefore, the application of the LL method to cover wider classes of SDEs is an appealing challenge. In particular, this paper focuses in the class of SDEs driven by (multiplicative) commutative noises. This class includes a number of well-known examples that have been studied in several applied fields, such as the stochastic Duffing–van der Pol oscillator, the noisy harmonic oscillators in potential wells and the stochastic Lorenz equations [13]. Specifically, the approach followed in this paper results from the combination of the LL technique and the above mentioned conjugacy property to define a LL scheme for the class of commutative noise SDEs. The implementation of the proposed LL scheme consists of two basic steps: (1) Local approximation of the conjugacy diffeomorfism through the solution of a piecewise pure-diffusion linear SDE driven by an Ornstein–Uhlenbeck process; and (2) Numerical solution of the piecewise conjugate RDE by the LL method given in [11].

The paper is organized as follows. Section 2 summaries the main results about the conjugacy between SDEs and RDEs that will be used throughout the paper. In Sections 3 and 4 the new numerical scheme is introduced for single-noise and commutative noise SDEs, respectively. Some implementation issues are also discussed in both sections. Finally, in Section 5, the performance of the new schemes is illustrated through three test examples.

2. Conjugacy of stochastic and random differential equations

Let $\mathbf{w}_t = (w_t^1, \dots, w_t^m)$ be a m-dimensional standard Wiener process and let

$$\mathrm{d}\mathbf{x}_t = \mathbf{f}_0(\mathbf{x}_t)\mathrm{d}t + \sum_{i=1}^{m} \mathbf{f}_i(\mathbf{x}_t) \circ \mathrm{d}w_t^i, \quad t \geqslant 0, \tag{1}$$

$$\mathbf{x}_{t_0} = \mathbf{x}_0 \tag{2}$$

be a Stratanovich SDE on $\mathbb{R}^d$ with vector fields $\mathbf{f}_0, \ldots, \mathbf{f}_m$ smooth enough and globally Lipschitz, so that its corresponding flow ϕ globally exists. Furthermore, assume that, for all $1 \leqslant i, j \leqslant m$, the Lie product

$$[\mathbf{f}_i, \mathbf{f}_j] = \frac{\partial \mathbf{f}_i}{\partial \mathbf{x}} \mathbf{f}_j - \frac{\partial \mathbf{f}_j}{\partial \mathbf{x}} \mathbf{f}_i$$

satisfies the commutativity condition

$$[\mathbf{f}_i, \mathbf{f}_j] = 0, \tag{3}$$

where $\frac{\partial \mathbf{f}_i}{\partial \mathbf{x}}$ denotes the partial derivative of $\mathbf{f}_i$ with respect to $\mathbf{x}$.

Let $\mathbf{u} : \mathbb{R}^m \times \mathbb{R}^d \to \mathbb{R}^d$ be the smooth vector field that satisfies

$$\begin{aligned} &\frac{\partial \mathbf{u}}{\partial z^i}(\mathbf{z}, \mathbf{x}) = \mathbf{f}_i(\mathbf{u}(\mathbf{z}, \mathbf{x})), \quad i = 1, \ldots, m, \\ &\mathbf{u}(\mathbf{0}, \mathbf{x}) = \mathbf{x} \end{aligned} \tag{4}$$

for $(\mathbf{z}, \mathbf{x}) \in \mathbb{R}^m \times \mathbb{R}^d$. In addition, let $\mathbf{\Phi}$ be the stationary diffeomorfism defined by $\mathbf{\Phi} = \mathbf{u}(\mathbf{z}_0, \cdot)$ and let $\mathbf{\Phi}_t, t \geqslant 0$ be the diffeomorfism on $\mathbb{R}^d$ that solves the pure-diffusion differential equation

$$\begin{aligned} &\mathrm{d}\mathbf{\Phi}_t = \sum_{i=1}^{m} \mathbf{f}_i(\mathbf{\Phi}_t) \circ \mathrm{d}z_t^i, \quad t \geqslant 0, \\ &\mathbf{\Phi}_0 = \mathbf{\Phi}, \end{aligned} \tag{5}$$

where

$$\mathrm{d}z_t^i = -\mu z_t^i \mathrm{d}t + \mathrm{d}w_t^i \tag{6}$$

is a stationary Ornstein–Uhlenbeck process, for all $i = 1, \ldots, m$, and $\mu > 0$. Then the following theorem states a conjugacy (defined through $\mathbf{\Phi}$) between the SDE (1) and a RDE.

Theorem 1 (Theorem 1.3 in [1]). *Let $(\chi_t)_{t \geqslant 0}$ be the flow on $\mathbb{R}^d$ generated by the random differential equation*

$$\mathrm{d}\mathbf{y}_t = g(\mathbf{z}_t, \mathbf{y}_t)\mathrm{d}t, \tag{7}$$

where

$$g(\mathbf{z}_t, \mathbf{y}_t) = \left(\frac{\partial \mathbf{\Phi}_t}{\partial \mathbf{x}} \right)^{-1} \left(\mathbf{f}_0(\mathbf{\Phi}_t \mathbf{y}_t) + \mu \sum_{i=1}^{m} \mathbf{f}_i(\mathbf{\Phi}_t \mathbf{y}_t) z_t^i \right)$$

and $\mathbf{z}_t = (z_t^1, \ldots, z_t^m)$. Then, for all $\mathbf{x} \in \mathbb{R}^d$

$$\phi_t(\mathbf{x}) = \mathbf{\Phi}_t \chi_t(\mathbf{\Phi}^{-1}\mathbf{x}), \tag{8}$$

where $(\phi_t)_{t \geqslant 0}$ denotes the flow of Eq. (1).

The following proposition gives an explicit expression for the solution $\mathbf{u}(\mathbf{z}, \mathbf{x})$ of the system (4). This, in turn, can be used to get explicit expressions for $\mathbf{\Phi}_t$ and $\mathbf{\Phi}$.

Proposition 2 (Proposition 5.1.10 in [14]). *The solution $\mathbf{u}(\mathbf{z}, \mathbf{x})$ of the system (4) is given by the composition in any order of the commutative flows $\xi_{z^1}^{\mathbf{f}_1}(\mathbf{x}), \xi_{z^2}^{\mathbf{f}_2}(\mathbf{x}), \ldots, \xi_{z^m}^{\mathbf{f}_m}(\mathbf{x})$, where for each $i = 1, \ldots, m$, the flow $\xi_{z^i}^{\mathbf{f}_i}(\mathbf{x})$ satisfies the ODE*

$$\begin{aligned} &\frac{\mathrm{d}\xi_{z^i}^{\mathbf{f}_i}(\mathbf{x})}{\mathrm{d}z^i} = \mathbf{f}_i(\xi_{z^i}^{\mathbf{f}_i}(\mathbf{x})), \\ &\xi_0^{\mathbf{f}_i}(\mathbf{x}) = \mathbf{x}. \end{aligned}$$

Besides,

$$\mathbf{u}(\mathbf{z}+\mathbf{z}',\cdot) = u(\mathbf{z},\cdot)\circ u(\mathbf{z}',\cdot) \tag{9}$$

and

$$(\mathbf{u}(\mathbf{z},\cdot))^{-1} = \mathbf{u}(-\mathbf{z},\cdot) \tag{10}$$

for all $\mathbf{z},\mathbf{z}' \in \mathbb{R}^m$.

In the next sections the solution $\mathbf{x}_t = \phi_t(\mathbf{x}_0)$ of (1) and (2) is approximated on the base of the conjugacy relationship (8). This requires the approximation of both, the corresponding conjugacy $\mathbf{\Phi}$ and the flow χ_t associated to RDE (7), which will be achieved through a local linearization approach.

3. Local linearization method for single-noise SDEs

Consider the single-noise SDE

$$\mathrm{d}\mathbf{x}_t = \mathbf{f}_0(\mathbf{x}_t)\mathrm{d}t + \mathbf{f}_1(\mathbf{x}_t)\circ \mathrm{d}w_t \tag{11}$$

with initial condition $\mathbf{x}_{t_0} = \mathbf{x}_0$. Let $(t)_h$ be a time partition defined as

$$(t)_h = \{0 = t_0 < t_1 < \cdots < t_n < \cdots\},$$

where

$$\sup_n (t_{n+1} - t_n) \leqslant h < 1.$$

For all $t_n \in (t)_h$, let $\mathbf{y}_{t_n} \in \mathbb{R}^d$ be a point close to $\mathbf{x}_{t_n}$, and consider the SDE

$$\mathrm{d}\mathbf{y}_t = \mathbf{f}_0(\mathbf{y}_t)\mathrm{d}t + (\mathbf{A}_1^{t_n}\mathbf{y}_t + \mathbf{b}_1^{t_n})\circ \mathrm{d}w_t, \quad t_n \leqslant t \leqslant t_{n+1} \tag{12}$$

with initial point $\mathbf{y}_{t_n}$, which is obtained from the local linear approximation (by first-order Taylor expansion) of the vector field $\mathbf{f}_1$ around $\mathbf{y}_{t_n}$. That is,

$$\mathbf{f}_1(\mathbf{y}_t) \approx \tilde{\mathbf{f}}_1(\mathbf{y}_t) = \mathbf{A}_1^{t_n}\mathbf{y}_t + \mathbf{b}_1^{t_n}, \quad t_n \leqslant t \leqslant t_{n+1},$$

where $\mathbf{A}_1^{t_n} = \frac{\partial \mathbf{f}_1}{\partial \mathbf{x}}(\mathbf{y}_{t_n})$ and $\mathbf{b}_1^{t_n} = \mathbf{f}_1(\mathbf{y}_{t_n}) - \mathbf{A}_1^{t_n}\mathbf{y}_{t_n}$. Then, according to the local linearization approach, the solution $\mathbf{y}_{t_{n+1}}$ of Eq. (12) at t_{n+1} defines a point closed to $\mathbf{x}_{t_{n+1}}$. In this way, starting with $\mathbf{y}_{t_0} = \mathbf{x}_{t_0}$, a sequence of points $\{\mathbf{y}_{t_n}\}$ is obtained as an approximation to $\{\mathbf{x}_{t_n}\}$. Equivalently, if ϕ_t and $\phi_t^{t_n}$ denote the flow of Eqs. (11) and (12), respectively, then

$$\phi_t(\mathbf{x}_{t_n}) \approx \phi_t^{t_n}(\mathbf{y}_{t_n}),$$

for all $t_n \in (t)_h$, $t \in [t_n, t_{n+1}]$, which defines the recursive expression

$$\mathbf{y}_{t_{n+1}} = \phi_{t_{n+1}}^{t_n}(\mathbf{y}_{t_n}). \tag{13}$$

for approximating $\mathbf{x}_{t_{n+1}}$. Moreover, according to Theorem 1

$$\phi_t^{t_n}(\mathbf{y}_{t_n}) = \mathbf{\Phi}_t^{t_n}\chi_t^{t_n}((\mathbf{\Phi}^{t_n})^{-1}\mathbf{y}_{t_n}), \quad t_n \leqslant t \leqslant t_{n+1}, \tag{14}$$

where $\chi_t^{t_n}$ is the flow generated by the random differential equation

$$\mathrm{d}\mathbf{v}_t = \mathbf{g}(\mathbf{v}_t, z_t)\mathrm{d}t, \quad t_n \leqslant t \leqslant t_{n+1} \tag{15}$$

with

$$\mathbf{g}(\mathbf{v}_t, z_t) := \left(\frac{\partial \Phi_t^{t_n}}{\partial \mathbf{x}}\right)^{-1}(\mathbf{f}_0(\mathbf{\Phi}_t^{t_n}\mathbf{v}_t) + \mu\tilde{\mathbf{f}}_1(\mathbf{\Phi}_t^{t_n}\mathbf{v}_t)z_t).$$

Besides, by Proposition 2, the conjugacy $\mathbf{\Phi}^{t_n}$ is a linear operator on $\mathbb{R}^d$ given by

$$\mathbf{\Phi}^{t_n}\mathbf{x} = \exp(\mathbf{A}_1^{t_n}z_{t_n})\mathbf{x} + \int_0^{z_{t_n}} \exp(\mathbf{A}_1^{t_n}(z_{t_n} - s))\mathbf{b}_1^{t_n}\,\mathrm{d}s$$

for $\mathbf{x} \in \mathbb{R}^d$, and so

$$\mathbf{\Phi}_t^{t_n}\mathbf{x} = \exp(\mathbf{A}_1^{t_n} z_t)\mathbf{x} + \int_0^{z_t} \exp(\mathbf{A}_1^{t_n}(z_t - s))\mathbf{b}_1^{t_n}\,\mathrm{d}s$$

for all $t \in [t_n, t_{n+1}]$. From (13) and (14) it follows that:

$$\mathbf{y}_{t_{n+1}} = \mathbf{\Phi}_{t_{n+1}}^{t_n}\chi_{t_{n+1}}^{t_n}((\mathbf{\Phi}^{t_n})^{-1}\mathbf{y}_{t_n}), \tag{16}$$

which equivalently defines the local linear approximation for $\mathbf{x}_{t_{n+1}}$ in term of the flow of the RDE (15).

With the change of variable $\mathbf{u}_t = \exp(\mathbf{A}_1^{t_n} z_{t_n})\mathbf{v}_t$ the recursion (16) can be rewritten as

$$\mathbf{y}_{t_{n+1}} = \mathbf{\Phi}_{t_{n+1}}^{t_n}\exp(-\mathbf{A}_1^{t_n} z_{t_n})\mathbf{u}_{t_{n+1}},$$

where the function $\mathbf{u}_t$ satisfies the RDE

$$\begin{aligned} \mathrm{d}\mathbf{u}_t &= \mathbf{q}_n(\mathbf{u}_t, z_t)\mathrm{d}t \\ \mathbf{u}_{t_n} &= \exp(\mathbf{A}_1^{t_n} z_{t_n})(\mathbf{\Phi}^{t_n})^{-1}\mathbf{y}_{t_n} \end{aligned} \tag{17}$$

for all $t \in [t_n, t_{n+1}]$, with

$$\begin{aligned} \mathbf{q}_n(\mathbf{u}_t, z_t) &= \exp(\mathbf{A}_1^{t_n} z_t)\mathbf{g}(\exp(-\mathbf{A}_1^{t_n} z_{t_n})\mathbf{u}_t, z_t) \\ &= \exp(-\mathbf{A}_1^{t_n}(z_t - z_{t_n}))[\mathbf{f}_0(\mathbf{\Phi}_t^{t_n}\exp(-\mathbf{A}_1^{t_n} z_{t_n})\mathbf{u}_t) + \mu\tilde{\mathbf{f}}_1(\mathbf{\Phi}_t^{t_n}\exp(-\mathbf{A}_1^{t_n} z_{t_n})\mathbf{u}_t)z_t]. \end{aligned}$$

If in addition

$$\mathbf{u}_{t_{n+1}} = \mathbf{u}_{t_n} + \mathbf{F}_n(\mathbf{u}_{t_n}, z_{t_n}; h_n), \quad h_n = t_{n+1} - t_n$$

denotes the approximated solution of Eq. (17) at $t = t_{n+1}$ given by a one-step explicit integrator, then the map (16) can be approximated by the map

$$\mathbf{y}_{n+1} = \mathbf{\Phi}_{n+1}^n[(\mathbf{\Phi}^n)^{-1}\mathbf{y}_n + \exp(-\mathbf{A}_1^n z_{t_n})\mathbf{F}_n(\exp(\mathbf{A}_1^n z_{t_n})(\mathbf{\Phi}^n)^{-1}\mathbf{y}_{t_n}, z_{t_n}; h_n)]$$

with the initial point $\mathbf{y}_0 = \mathbf{y}_{t_0}$, where

$$\mathbf{\Phi}^n\mathbf{x} = \exp(\mathbf{A}_1^n z_{t_n})\mathbf{x} + \int_0^{z_{t_n}} \exp(\mathbf{A}_1^n(z_{t_n} - s))\mathbf{b}_1^n\,\mathrm{d}s, \quad \mathbf{x} \in \mathbb{R}^d,$$

$\mathbf{A}_1^n = \frac{\partial \mathbf{f}_1}{\partial \mathbf{x}}(\mathbf{y}_n)$, $\mathbf{b}_1^n = \mathbf{f}_1(\mathbf{y}_n) - \mathbf{A}_1^n\mathbf{y}_n$ and

$$\mathbf{\Phi}_{n+1}^n\mathbf{x} = \exp(\mathbf{A}_1^n z_{t_{n+1}})\mathbf{x} + \int_0^{z_{t_{n+1}}} \exp(\mathbf{A}_1^n(z_{t_{n+1}} - s))\mathbf{b}_1^n\,\mathrm{d}s, \quad \mathbf{x} \in \mathbb{R}^d.$$

From the linearity of $\mathbf{\Phi}_{n+1}^n$ follows that:

$$\mathbf{y}_{n+1} = \mathbf{\Phi}_{n+1}^n(\mathbf{\Phi}^n)^{-1}\mathbf{y}_n + \exp(\mathbf{A}_1^n\Delta z_n)\mathbf{F}_n(\exp(\mathbf{A}_1^n z_{t_n})(\mathbf{\Phi}^n)^{-1}\mathbf{y}_{t_n}, z_{t_n}; h_n),$$

whereas from properties (9) and (10) it is obtained

$$\mathbf{y}_{n+1} = \exp(\mathbf{A}_1^n\Delta z_n)\mathbf{y}_n + \int_0^{\Delta z_n} \exp(\mathbf{A}_1^n(\Delta z_n - s))\mathbf{b}_1^n\,\mathrm{d}s + \exp(\mathbf{A}_1^n\Delta z_n)\mathbf{F}_n(\exp(\mathbf{A}_1^n z_{t_n})(\mathbf{\Phi}^n)^{-1}\mathbf{y}_{t_n}, z_{t_n}; h_n),$$

where $\Delta z_n := z_{t_{n+1}} - z_{t_n}$. Moreover, by using the identity

$$\int_0^{\Delta z_n} \exp(\mathbf{A}_1^n(\Delta z_n - s))\mathbf{A}_1^n\,\mathrm{d}s = \exp(\mathbf{A}_1^n\Delta z_n) - \mathbf{I}_d \tag{18}$$

it is obtained

$$\mathbf{y}_{n+1} = \mathbf{y}_n + \int_0^{\Delta z_n} \exp(\mathbf{A}_1^n(\Delta z_n - s))\mathbf{f}_1(\mathbf{y}_n)\,\mathrm{d}s + \exp(\mathbf{A}_1^n\Delta z_n)\mathbf{F}_n(\exp(\mathbf{A}_1^n z_{t_n})(\mathbf{\Phi}^n)^{-1}\mathbf{y}_n, z_{t_n}; h_n),$$

which provides an approximation to $\mathbf{x}_{t_{n+1}}$ in terms of an approximation to the flow of the RDE (17). Here, $\mathbf{I}_d$ denotes the d-dimensional identity matrix.

In principle, any numerical method for RDEs can be used. For instance, the well-known Euler scheme for Eq. (15) gives [15,16]

$$\mathbf{F}_n(\exp(\mathbf{A}_1^n z_{t_n})(\boldsymbol{\Phi}^n)^{-1}\mathbf{y}_n, z_{t_n}; h_n) = h_n(\mathbf{f}_0(\mathbf{y}_n) + \mu\mathbf{f}_1(\mathbf{y}_n)z_{t_n})$$

However, the simulation results presented in [11] indicated that the LL scheme has better performance than Euler and Heun schemes for approximating the dynamics of nonlinear RDEs. Thus, the choice of the LL scheme for Eq. (15) is in order. According to Section 2 in [11], the LL scheme gives

$$\mathbf{F}_n(\exp(\mathbf{A}_1^n z_{t_n})(\boldsymbol{\Phi}^n)^{-1}\mathbf{y}_n, z_{t_n}; h_n) = \mathbf{L}_0\exp(\mathbf{C}_n h_n)\mathbf{R}_0,$$

where

$$\mathbf{C}_n = \begin{pmatrix} \frac{\partial \mathbf{F}_n}{\partial \mathbf{u}}(\mathbf{u}_n, z_{t_n}) & \frac{\partial \mathbf{F}_n}{\partial z_t}(\mathbf{u}_n, z_{t_n})\frac{\Delta z_n}{h_n} & \mathbf{F}_n(\mathbf{u}_n, z_{t_n}) \\ \mathbf{0} & 0 & 1 \\ \mathbf{0} & 0 & 0 \end{pmatrix} \in \mathbb{R}^{(d+2)\times(d+2)},$$

$\mathbf{L}_0 = [\mathbf{I}_d \mathbf{0}_{d\times 2}]$ and $\mathbf{R}_0 = [\mathbf{0}_{1\times(d+1)} 1]^{\mathrm{T}}$, with

$$\mathbf{u}_n = \exp(\mathbf{A}_1^n z_{t_n})(\boldsymbol{\Phi}^n)^{-1}\mathbf{y}_n$$
$$\mathbf{F}_n(\mathbf{u}_n, z_{t_n}) = \mathbf{f}_0(\mathbf{y}_n) + \mu\mathbf{f}_1(\mathbf{y}_n)z_{t_n},$$
$$\frac{\partial \mathbf{F}_n}{\partial \mathbf{u}}(\mathbf{u}_n, z_{t_n}) = \mathbf{A}_0^n + \mu\mathbf{A}_1^n z_{t_n},$$
$$\frac{\partial \mathbf{F}_n}{\partial z_t}(\mathbf{u}_n, z_{t_n}) = \mathbf{A}_0^n\mathbf{f}_1(\mathbf{y}_n) - \mathbf{A}_1^n\mathbf{f}_0(\mathbf{y}_n) + \mu\mathbf{f}_1(\mathbf{y}_n)$$

and $\mathbf{A}_0^n = \frac{\partial \mathbf{f}_0}{\partial \mathbf{x}}(\mathbf{y}_n)$. Therefore,

$$\mathbf{y}_{n+1} = \mathbf{y}_n + \int_0^{\Delta z_n} \exp(\mathbf{A}_1^n(\Delta z_n - s))\mathbf{f}_1(\mathbf{y}_n)\mathrm{d}s + \exp(\mathbf{A}_1^n\Delta z_n)\mathbf{L}_0\exp(\mathbf{C}_n h_n)\mathbf{R}_0,$$

which by Theorem 1 in [17] can be rewritten as

$$\mathbf{y}_{n+1} = \mathbf{y}_n + \mathbf{L}_1\exp(\mathbf{D}_n\Delta z_n)\mathbf{R}_1 + \exp(\mathbf{A}_1^n\Delta z_n)\mathbf{L}_0\exp(\mathbf{C}_n h_n)\mathbf{R}_0, \tag{19}$$

where

$$\mathbf{D}_n = \begin{pmatrix} \mathbf{A}_1^n & \mathbf{f}_1(\mathbf{y}_n) \\ \mathbf{0} & 0 \end{pmatrix} \in \mathbb{R}^{(d+1)\times(d+1)},$$

$\mathbf{L}_1 = [\mathbf{I}_d \mathbf{0}_{d\times 1}]$ and $\mathbf{R}_1 = [\mathbf{0}_{1\times d} 1]^{\mathrm{T}}$. The recursive expression (19) defines finally the conjugated LL approximation to the solution of the single-noise SDE (11) for all $t_n \in (t)_h$.

For computational purposes and according to Theorem 1 in [17] the above scheme can be rewritten as

$$\mathbf{y}_{n+1} = \mathbf{y}_n + \mathbf{v}_1(\mathbf{y}_n) + \mathbf{B}(\mathbf{y}_n)\mathbf{v}_2(\mathbf{y}_n), \tag{20}$$

where the d-dimensional vectors $\mathbf{v}_1(\mathbf{y}_n)$, $\mathbf{v}_2(\mathbf{y}_n)$ and the $d \times d$ matrix $\mathbf{B}(\mathbf{y}_n)$ are defined in the following block matrices:

$$\begin{pmatrix} \mathbf{B}(\mathbf{y}_n) & \mathbf{v}_1(\mathbf{y}_n) \\ - & - \end{pmatrix} = \exp(\mathbf{D}_n\Delta z_n) \quad \text{and} \quad \begin{pmatrix} - & \mathbf{v}_2(\mathbf{y}_n) \\ - & - \end{pmatrix} = \exp(\mathbf{C}_n h_n).$$

It is obvious that the main computational task for implementing the scheme (20) is the computation of matrix exponentials. A number of algorithms are available for this purpose. For instance, those based on rational Padé approximations, the Schur decomposition or Krylov subspace methods (see [18,19] for excellent reviews). The choice of one of them will mainly depend on the size and structure of the matrices $\mathbf{C}_n$ and $\mathbf{D}_n$ in (20). For high dimensional matrices, Krylov subspace methods are strongly recommended. For matrices of certain special structures, several algorithms are presented in [20]. Nowadays, professional mathematical softwares, such as MATLAB, provide efficient codes that implement a number of such algorithms. On this basis, the numerical evaluation of the scheme under consideration can be carried out in an effective, accurate and simple way.

Similar implementations for computing the LL method for ODEs and SDEs have been elaborated in [21], where more details about related issues can be found.

4. Local linearization method for commutative noise case

The approach followed in the previous section can be directly extended to more general equations. So, consider the commutative noise SDE

$$\begin{aligned} d\mathbf{x}_t &= \mathbf{f}_0(\mathbf{x}_t)dt + \sum_{i=1}^{m} \mathbf{f}_i(\mathbf{x}_t) \circ dw_t^i, \\ \mathbf{x}_{t_0} &= \mathbf{x}_0 \end{aligned} \tag{21}$$

with $m > 1$. For this, in addition to the commutative condition (3), suppose that

$$\frac{\partial \mathbf{f}_i}{\partial \mathbf{x}} \frac{\partial \mathbf{f}_j}{\partial \mathbf{x}} - \frac{\partial \mathbf{f}_j}{\partial \mathbf{x}} \frac{\partial \mathbf{f}_i}{\partial \mathbf{x}} = 0 \tag{22}$$

also holds, for all $1 \leqslant i, j \leqslant m$ and $\mathbf{x} \in \mathbb{R}^d$.

Conditions (3) and (22) are required for applying the conjugacy Theorem 1 to the local linear approximations of Eq. (21). It is worth to note that there is a number of classes of SDEs satisfying both assumptions. Example are the d-dimensional systems of the form

$$dx_t^i = a^i(x_t^1, .., x_t^d)dt + b^i(x_t^i)dw_t^i, \quad i = 1 \ldots d$$

and

$$\begin{aligned} dx_t^i &= a^i(x_t^1, \ldots, x_t^d)dt, \quad i = 1 \ldots d-1, \\ dx_t^d &= a^d(x_t^1, \ldots, x_t^d)dt + \sum_{j=1}^{m} b^j(x_t^1, \ldots, x_t^d)dw_t^j, \end{aligned}$$

which include a number of well-known equations such as Shiga model [28] in the framework of genetics and the general stochastic Duffing–van der Pol oscillator considered in [29], just for mention a few.

Similarly to the previous section, the LL scheme will be obtained from the linearization of the vector fields $\mathbf{f}_i$ around each point $\mathbf{y}_{t_n} \in \mathbb{R}^d$ closed to $\mathbf{x}_{t_n}$. That is,

$$\mathbf{f}_i(\mathbf{x}_t) \approx \tilde{\mathbf{f}}_i(\mathbf{x}_t) = \mathbf{A}_i^{t_n}\mathbf{x}_t + \mathbf{b}_i^{t_n}, \quad t_n \leqslant t \leqslant t_{n+1}$$

for all $t_n \in (t)_h$ and $i = 1, .., m$, where $\mathbf{A}_i^{t_n} = \frac{\partial \mathbf{f}_i}{\partial \mathbf{x}}(\mathbf{y}_{t_n})$ and $\mathbf{b}_i^{t_n} = \mathbf{f}_i(\mathbf{y}_{t_n}) - \mathbf{A}_i^{t_n}\mathbf{y}_{t_n}$. Thus, according to the local linearization approach, the solution $\mathbf{y}_{t_{n+1}}$ of the equation

$$d\mathbf{y}_t = \mathbf{f}_0(\mathbf{y}_t)dt + \sum_{i=1}^{m} \tilde{\mathbf{f}}_i(\mathbf{y}_t) \circ dw_t, \quad t_n \leqslant t \leqslant t_{n+1} \tag{23}$$

at t_{n+1} defines a point closed to $\mathbf{x}_{t_{n+1}}$.

It is easy to see that conditions (3) and (22) guarantee the commutativity of the vector fields $\tilde{\mathbf{f}}_i$ as well, i.e. the linear SDE (23) is also driven by commutative noise. Therefore, Theorem 1 applied to (23) yields to the approximation

$$\phi_t(\mathbf{x}_{t_n}) \approx \phi_t^{t_n}(\mathbf{y}_{t_n}) := \mathbf{\Phi}_t^{t_n}\chi_t^{t_n}((\mathbf{\Phi}^{t_n})^{-1}\mathbf{y}_{t_n}), \quad t_n \leqslant t \leqslant t_{n+1}$$

between the flow ϕ_t of the SDEs (21) and the flow $\chi_t^{t_n}$ of the piecewise RDE

$$d\mathbf{y}_t = \left(\frac{\partial \mathbf{\Phi}_t^{t_n}}{\partial \mathbf{x}}\right)^{-1} \left(\mathbf{f}_0(\mathbf{\Phi}_t^{t_n}\mathbf{y}_t) + \mu \sum_{i=1}^{m} \tilde{\mathbf{f}}_i(\mathbf{\Phi}_t^{t_n}\mathbf{y}_t)z_t^i\right)dt, \quad t_n \leqslant t \leqslant t_{n+1}.$$

In this case, Proposition 2 gives

$$\mathbf{\Phi}^{t_n}\mathbf{x} = \xi_{z_{t_n}^1}^{\mathbf{f}_1, t_n} \circ \xi_{z_{t_n}^2}^{\mathbf{f}_2, t_n} \circ \cdots \circ \xi_{z_{t_n}^m}^{\mathbf{f}_m, t_n}(\mathbf{x})$$

and

$$\mathbf{\Phi}_t^{t_n}\mathbf{x} = \xi_{z_t^1}^{\mathbf{f}_1,t_n} \circ \xi_{z_t^2}^{\mathbf{f}_2,t_n} \circ \cdots \circ \xi_{z_t^m}^{\mathbf{f}_m,t_n}(\mathbf{x})$$

with

$$\xi_{z_t^i}^{\mathbf{f}_i,t_n} = \exp(\mathbf{A}_i^{t_n} z_t^i)\mathbf{x} + \int_0^{z_t^i} \exp(\mathbf{A}_i^{t_n}(z_t^i - s))\mathbf{b}_i^{t_n}\,\mathrm{d}s.$$

Similarly to the previous section, it can be seen that the expression

$$\mathbf{y}_{t_{n+1}} = \mathbf{\Phi}_{t_{n+1}}^{t_n} \exp\left(-\sum_{i=1}^m \mathbf{A}_i^{t_n} z_{t_n}^i\right)\mathbf{u}_{t_{n+1}}$$

provides an approximation to $\mathbf{x}_{t_n}$, for all $t_n \in (t)_h$, where the function $\mathbf{u}_t$ satisfies the RDE

$$\begin{aligned} \mathrm{d}\mathbf{u}_t &= \mathbf{q}_n(\mathbf{u}_t, \mathbf{z}_t)\mathrm{d}t \\ \mathbf{u}_{t_n} &= \exp\left(\sum_{i=1}^m \mathbf{A}_i^{t_n} z_{t_n}\right)(\mathbf{\Phi}^{t_n})^{-1}\mathbf{y}_{t_n} \end{aligned} \tag{24}$$

for all $t \in [t_n, t_{n+1}]$, with

$$\begin{aligned} \mathbf{q}_n(\mathbf{u}_t, z_t) &= \exp\left(\sum_{i=1}^m \mathbf{A}_i^{t_n} z_{t_n}^i\right)\mathbf{g}\left(\exp\left(-\sum_{i=1}^m \mathbf{A}_i^{t_n} z_{t_n}^i\right)\mathbf{u}_t, \mathbf{z}_t\right) \\ &= \exp(-\sum_{i=1}^m \mathbf{A}_i^{t_n}(z_t^i - z_{t_n}^i))\left[\mathbf{f}_0\left(\mathbf{\Phi}_t^{t_n} \exp\left(-\sum_{i=1}^m \mathbf{A}_i^{t_n} z_{t_n}^i\right)\mathbf{u}_t\right) + \mu \sum_{j=1}^m \tilde{\mathbf{f}}_i(\mathbf{\Phi}_t^{t_n} \exp\left(-\sum_{i=1}^m \mathbf{A}_i^{t_n} z_{t_n}^i\right)\mathbf{u}_t) z_t^i\right]. \end{aligned}$$

Moreover, if a one-step map $\mathbf{F}_n$ is defined as in the previous section, it is obtained the recursion

$$\mathbf{y}_{n+1} = \mathbf{\Phi}_{n+1}^n(\mathbf{\Phi}^n)^{-1}\mathbf{y}_n + \exp\left(\sum_{i=1}^m \mathbf{A}_i^n \Delta z_n^i\right)\mathbf{F}_n\left(\exp\left(\sum_{i=1}^m \mathbf{A}_i^n z_{t_n}^i\right)(\mathbf{\Phi}^n)^{-1}\mathbf{y}_n, \mathbf{z}_{t_n}; h_n\right)$$

with initial point $\mathbf{y}_0 = \mathbf{y}_{t_0}$, where

$$\mathbf{\Phi}_{n+1}^n\mathbf{x} = \xi_{z_{t_{n+1}}^1}^{\mathbf{f}_1,n} \circ \xi_{z_{t_{n+1}}^2}^{\mathbf{f}_2,n} \circ \cdots \circ \xi_{z_{t_{n+1}}^m}^{\mathbf{f}_m,n}(\mathbf{x})$$

and $\mathbf{\Phi}^n := \mathbf{\Phi}_n^n$, with

$$\xi_{z_{t_{n+1}}^i}^{\mathbf{f}_i,n} = \exp(\mathbf{A}_i^n z_{t_{n+1}}^i)\mathbf{x} + \int_0^{z_{t_{n+1}}^i} \exp(\mathbf{A}_i^n(z_{t_{n+1}}^i - s))\mathbf{b}_i^n\,\mathrm{d}s,$$

$\mathbf{A}_i^n = \frac{\partial \mathbf{f}_i}{\partial \mathbf{x}}(\mathbf{y}_n)$, $\mathbf{b}_i^n = \mathbf{f}_i(\mathbf{y}_n) - \mathbf{A}_i^n\mathbf{y}_n$ and $\Delta z_n^i = z_{t_{n+1}}^i - z_{t_n}^i$. Again, by using (9), (10) and (18) follows that:

$$\begin{aligned} \mathbf{y}_{n+1} &= \xi_{\Delta z_n^1}^{\mathbf{f}_1,n} \circ \xi_{\Delta z_n^2}^{\mathbf{f}_2,n} \circ \cdots \circ \xi_{\Delta z_n^m}^{\mathbf{f}_m,n}(\mathbf{y}_n) + \exp\left(\sum_{i=1}^m \mathbf{A}_i^n \Delta z_n^i\right)\mathbf{F}_n(\exp\left(\sum_{i=1}^m \mathbf{A}_i^n z_{t_n}^i\right)(\Phi^n)^{-1}\mathbf{y}_n, \mathbf{z}_{t_n}; h_n) \\ &= \mathbf{y}_n + \sum_{i=1}^m \exp\left(\sum_{j=1}^{i-1} \mathbf{A}_j^n \Delta z_n^j\right)\int_0^{\Delta z_n^i} \exp(\mathbf{A}_i^n(\Delta z_n^i - s))\mathbf{f}_i(\mathbf{y}_n)\mathrm{d}s \\ &\quad + \exp\left(\sum_{i=1}^m \mathbf{A}_i^n \Delta z_n^i\right)\mathbf{F}_n\left(\exp\left(\sum_{i=1}^m \mathbf{A}_i^n z_{t_n}^i\right)(\mathbf{\Phi}^n)^{-1}\mathbf{y}_n, \mathbf{z}_{t_n}; h_n\right). \end{aligned}$$

Finally, as in the previous section, if the LL scheme is used to approximate the solution of RDE (24) then

$$\mathbf{F}_n\left(\exp\left(\sum_{i=1}^m \mathbf{A}_i^n z_{t_n}^i\right)(\mathbf{\Phi}^n)^{-1}\mathbf{y}_n, \mathbf{z}_{t_n}; h_n\right) = \mathbf{L}_0 \exp(\mathbf{C}_n h_n)\mathbf{R}_0,$$

where

$$\mathbf{C}_n = \begin{pmatrix} \frac{\partial \mathbf{q}_n}{\partial \mathbf{u}}(\mathbf{u}_n, z_{t_n}) & \sum_{j=1}^{m} \frac{\partial \mathbf{q}_n}{\partial z^j}(\mathbf{u}_n, z_{t_n})\frac{\Delta z_n^j}{h_n} & \mathbf{q}_n(\mathbf{u}_n, z_{t_n}) \\ \mathbf{0} & 0 & 1 \\ \mathbf{0} & 0 & 0 \end{pmatrix} \in \mathbb{R}^{(d+2)\times(d+2)}$$

with

$$\begin{aligned}
\mathbf{u}_n &= \exp\left(\sum_{i=1}^{m} \mathbf{A}_i^n z_{t_n}^i\right)(\mathbf{\Phi}^n)^{-1}\mathbf{y}_n, \\
\mathbf{q}_n(\mathbf{u}_n, z_{t_n}) &= \mathbf{f}_0(\mathbf{y}_n) + \mu \sum_{i=1}^{m} \mathbf{f}_i(\mathbf{y}_n) z_{t_n}^i, \\
\frac{\partial \mathbf{q}_n}{\partial \mathbf{u}}(\mathbf{u}_n, z_{t_n}) &= \mathbf{A}_0^n + \mu \sum_{i=1}^{m} \mathbf{A}_i^n z_{t_n}^i, \\
\frac{\partial \mathbf{q}_n}{\partial z^j}(\mathbf{u}_n, z_{t_n}) &= \mathbf{A}_0^n \mathbf{f}_j(\mathbf{y}_n) - \mathbf{A}_j^n \mathbf{f}_0(\mathbf{y}_n) + \mu \mathbf{f}_j(\mathbf{y}_n)
\end{aligned}$$

and $\mathbf{A}_0^n = \frac{\partial \mathbf{f}_0}{\partial \mathbf{x}}(\mathbf{y}_n)$. In this way, the recursive expression

$$\mathbf{y}_{n+1} = \mathbf{y}_n + \sum_{i=1}^{m} \exp\left(\sum_{j=1}^{i-1} \mathbf{A}_j^n \Delta z_n^j\right)\mathbf{L}_1 \exp(\mathbf{D}_n^i \Delta z_n^i)\mathbf{R}_1 + \exp\left(\sum_{i=1}^{m} \mathbf{A}_i^n \Delta z_n^i\right)\mathbf{L}_0 \exp(\mathbf{C}_n h_n)\mathbf{R}_0 \tag{25}$$

with initial point $\mathbf{y}_0 = \mathbf{x}_0$, defines the conjugated LL approximation to the solution of the commutative noise SDE (21), for all $t_n \in (t)_h$, where

$$\mathbf{D}_n^i = \begin{pmatrix} \mathbf{A}_i^n & \mathbf{f}_i(\mathbf{y}_n) \\ \mathbf{0} & 0 \end{pmatrix} \in \mathbb{R}^{(d+1)\times(d+1)}$$

and $\mathbf{L}_0$, $\mathbf{L}_1$, $\mathbf{R}_0$, $\mathbf{R}_1$ are defined as in the previous section.

For computational purposes, Theorem 1 in [17] yields to the scheme

$$\mathbf{y}_{n+1} = \mathbf{y}_n + \sum_{i=1}^{m}\left(\prod_{j=1}^{i-1} \mathbf{B}^j(\mathbf{y}_n)\right)\mathbf{v}_1^i(\mathbf{y}_n) + \prod_{i=1}^{m} \mathbf{B}^i(\mathbf{y}_n)\mathbf{v}_2(\mathbf{y}_n),$$

where the d-dimensional vectors $\mathbf{v}_1^i(\mathbf{y}_n)$, $\mathbf{v}_2(\mathbf{y}_n)$ and the $d \times d$ matrices $\mathbf{B}^i(\mathbf{y}_n)$ are defined by the following block matrices:

$$\begin{pmatrix} \mathbf{B}^i(\mathbf{y}_n) & \mathbf{v}_1^i(\mathbf{y}_n) \\ - & - \end{pmatrix} = \exp(\mathbf{D}_n^i \Delta z_n) \quad \text{and} \quad \begin{pmatrix} - & \mathbf{v}_2(\mathbf{y}_n) \\ - & - \end{pmatrix} = \exp(\mathbf{C}_n h_n).$$

5. Numerical simulations

In this section the performance of the LL method is illustrated by means of three test examples. In all examples, the parameter μ of the Ornstein–Uhlenbeck process z_t was chosen as $\mu = 1$. The first one corresponds to the stochastic Duffing–van der Pol oscillator with a single multiplicative noise in the position, which is described by the stochastic differential equation

$$\begin{aligned}
\mathrm{d}x_1 &= x_2\,\mathrm{d}t, \\
\mathrm{d}x_2 &= (-\alpha x_1 + \beta x_2 - x_1^2(x_1 + x_2))\mathrm{d}t + \sigma x_1 \circ \mathrm{d}w_t, \\
x_1(0) &= x_2(0) = 1,
\end{aligned} \tag{26}$$

where β is the damping parameter, α the parameter controlling the strength of the restoring force and σ is the intensity of the noise. A number of works have been carried out for studying the dynamical behavior of this equation (see [22] and references therein). Of particular interest has been the investigation of the stochastic bifurcation scenario of this system [23]. It is well-known that the deterministic Duffing–van der Pol oscillator ($\sigma = 0$) exhibits a Hopf bifurcation for the value $\beta = 0$ (considered as bifurcation parameter) and fixed α. That is, the fixed point $(x_1, x_2) = (0, 0)$ is a global attractor for $\beta \leqslant 0$ and becomes unstable for $\beta > 0$, where the new attractor takes the form of a topological disc. Formally, the Hopf bifurcation can be investigated by analyzing the two eigenvalues of the linearization at zero as functions of the parameter β.

In the stochastic case the analysis is rather complicated. Indeed, the above mentioned eigenvalues need to be replaced by the Lyapunov exponents of the SDE (26). In this case the origin remains as a stable fixed point as long as the top Lyapunov exponent λ_1 (as function of the bifurcation parameter β) be negative. Hence, stability is lost when λ_1 becomes positive and two different qualitative behavior emerges, which depends on the sign of the second Lyapunov exponent λ_2. The simulation results presented in this section focus on the three different qualitative scenarios given by the conditions $\lambda_2 < 0 < \lambda_1$, $\lambda_2 < \lambda_1 < 0$ and $0 < \lambda_2 < \lambda_1$, respectively. As in the deterministic case, the second scenario corresponds to a global attractor $(x_1, x_2) = (0, 0)$. The case $\lambda_2 < 0 < \lambda_1$ is associated with the hyperbolic (saddle) scenario and for the third one the fixed point (0,0) is a repealer, leading to a topological disc type global attractor.

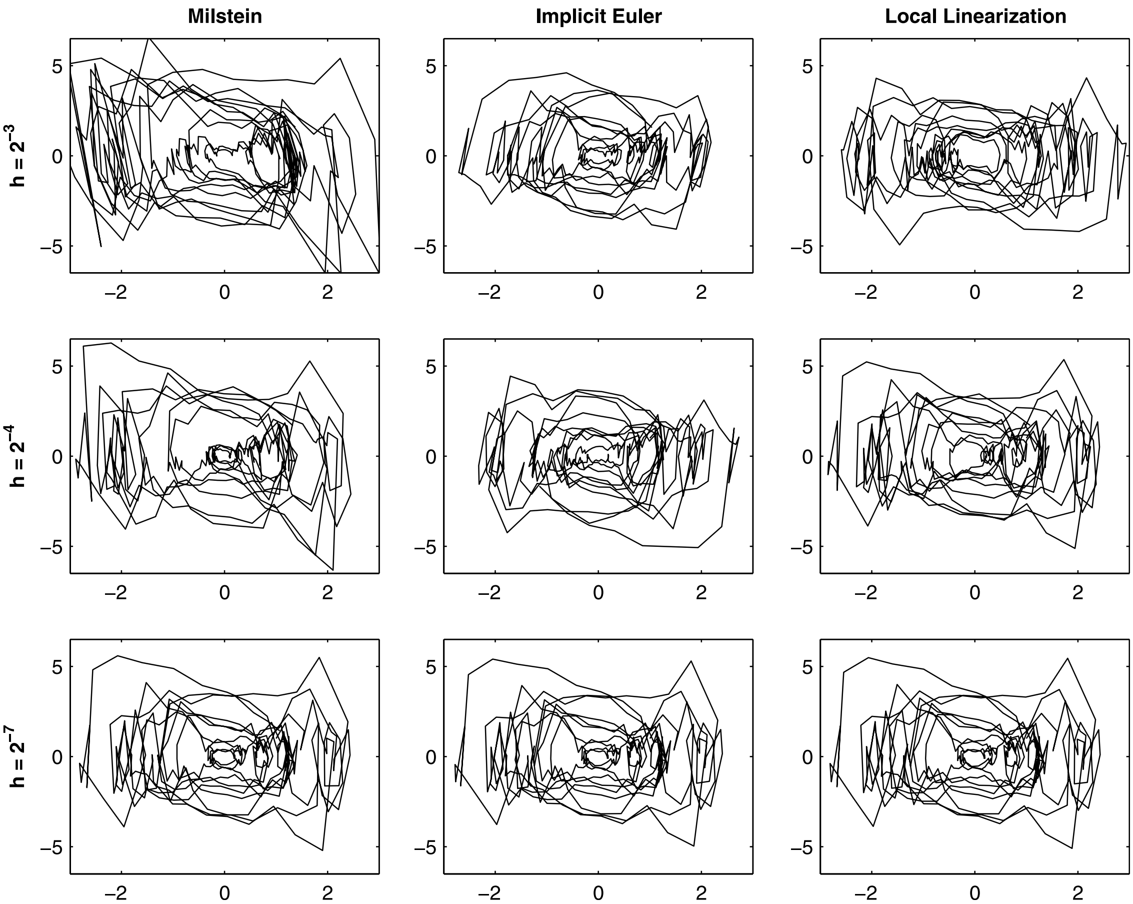

Fig. 1. Comparison of the Milstein, implicit Euler and local linearization schemes in the integration of Eq. (26), with values $\sigma = 3$, $\beta = -0.5$, $\alpha = 0.25$ corresponding to the strange attractor type scenario ($\lambda_2 < 0 < \lambda_1$). For each scheme, the phase-portraits show the approximations obtained with step-sizes $h = 2^{-3}, 2^{-4}, 2^{-7}$.

The simulations below are going to show the performance of the introduced LL method in these three different qualitative scenarios. For this purpose, the value of the parameter is chosen as $\alpha = |\beta|^2$, for which it is known from [24] that

$$\lambda_1 = \beta + \frac{\gamma^{1/3}}{2} 12^{1/3} \frac{\Gamma\left(\frac{1}{2}\right)}{\Gamma\left(\frac{1}{6}\right)},$$

$$\lambda_2 = \beta - \frac{\gamma^{1/3}}{2} 12^{1/3} \frac{\Gamma\left(\frac{1}{2}\right)}{\Gamma\left(\frac{1}{6}\right)},$$

with $\gamma = \frac{\sigma^2}{2}$. Hence, by fixing σ, the three scenarios can be reproduced by a suitable choice of the parameter β. Three different combination of these parameters were used for the integration of the system (26) on $0 \leqslant t \leqslant 50$.

Fig. 1 shows the comparison among the Milstein scheme, the implicit Euler scheme and the LL scheme (20) for the hyperbolic fixed point scenario ($\lambda_2 < 0 < \lambda_1$), corresponding to the values $\sigma = 3$, $\beta = -0.5$ and $\alpha = 0.25$. Rows correspond to approximations obtained with different step-sizes $h = 2^{-3}, 2^{-4}, 2^{-7}$. For the sake of comparison, in this and in the figures below, all phase-portraits are plotted at the same discrete times associated with the coarsest partition $(t)_{h_{\max}}$, where $h_{\max} = 2^{-3}$. It is seen that all the plots in the right column are more similar to those in the last row, which evidences the well performance of the LL method even for the moderately large step size $h = 2^{-3}$. Notice that the explicit Milstein scheme (first column) shows the poorest performance.

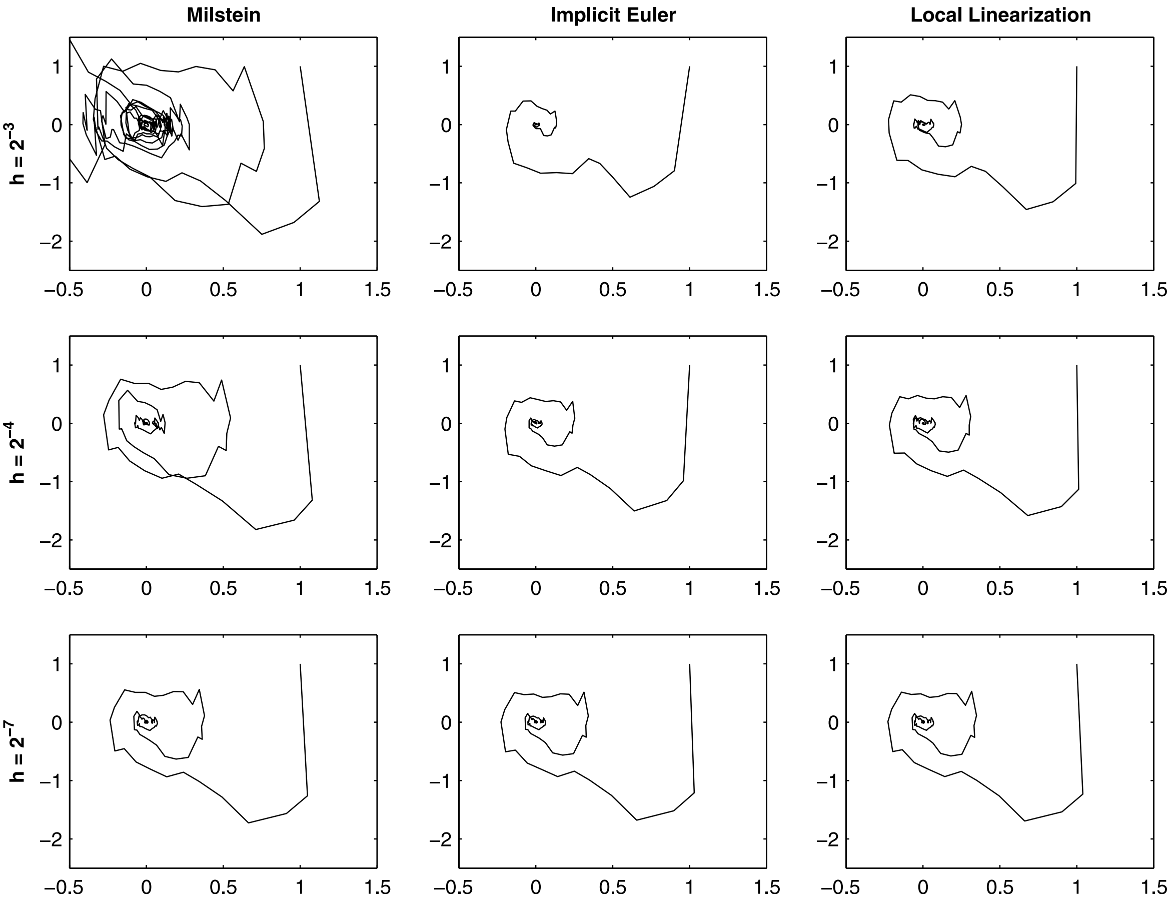

Fig. 2. Trajectories of the Milstein, implicit Euler and local linearization schemes around the fixed point $(0,0)$, corresponding to the scenario ($\lambda_2 < \lambda_1 < 0$) of the system (26) with parameters $\sigma = 3$, $\beta = -1.2$, and $\alpha = 1.44$. For each scheme, the phase-portraits show the approximations obtained with step-sizes $h = 2^{-3}, 2^{-4}, 2^{-7}$.

Fig. 2 shows the trajectories obtained by said three schemes around the asymptotically stable fixed point (0,0) (corresponding to $\lambda_2 < \lambda_1 < 0$). In this case the parameters of the Eq. (26) were chosen as $\sigma = 3$, $\beta = -1.2$ and $\alpha = 1.44$. As in Fig. 1, the Milstein scheme does not perform well for the largest step size $h = 2^{-3}$ in comparison with the implicit Euler and LL schemes. Also notice that even for large step-sizes $h = 2^{-3}$ and $h = 2^{-4}$, the LL scheme correctly reproduces fine details of the exact solution around the stable fixed point.

Fig. 3 shows the repealer fixed point scenario ($0 < \lambda_2 < \lambda_1$) corresponding to $\sigma = 3$, $\beta = 2$, and $\alpha = 4$. Notice that the approximation provided by the Milstein scheme does not reconstruct at all the actual dynamics of the system. In fact, this provides an approximation that explodes at time $t = 9$. In contrast, the LL method shows a well performance for all step sizes.

It can be concluded from these figures that the behavior of the LL scheme is very similar to that of the implicit Euler scheme for all step sizes. However, the implicit Euler scheme requires much more computational effort than the LL method. This is demonstrated in Table 1, which shows the relative CPU time for each numerical scheme with respect to the explicit Milstein scheme. Notice that the CPU time for the LL method is around 30 times lower than that for the implicit Euler method.

The second example is the stochastic planar Brusselator [25]

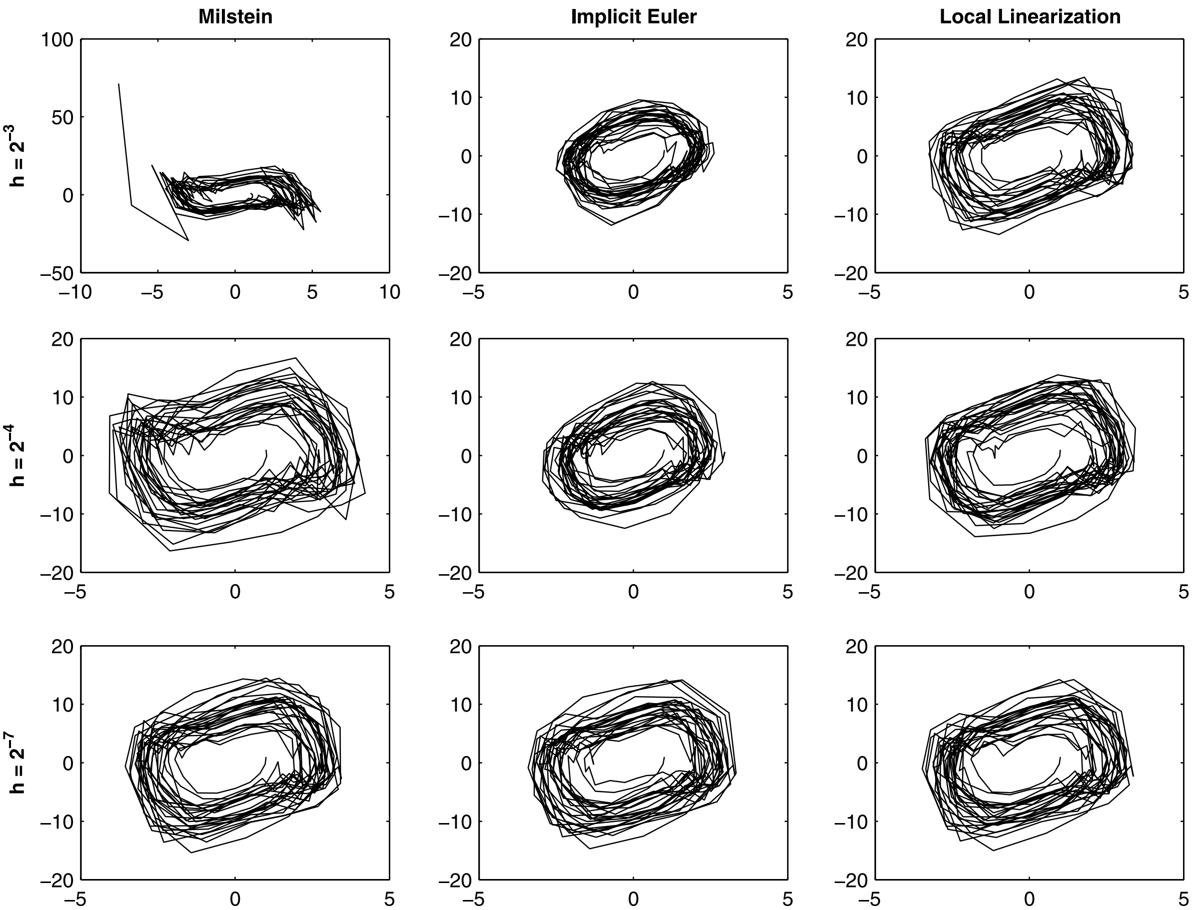

Fig. 3. Comparison of the Milstein, implicit Euler and local linearization scheme in the integration of Eq. (26), with values $\sigma = 3$, $\beta = 2$ and $\alpha = 4$ corresponding to the limit cycle scenario ($0 < \lambda_2 < \lambda_1$). For each scheme, the phase-portraits show the approximations obtained with step-sizes $h = 2^{-3}, 2^{-4}, 2^{-7}$.

Table 1
Relative CPU times for different numerical schemes

Scheme	Milstein	Local linearization	Implicit Euler
Relative CPU time	1	2.8396	85.7914

$$\begin{aligned} \mathrm{d}x_1 &= [(a-1)x_1 + ax_1^2 + (1+x_1)^2 x_2]\mathrm{d}t + \sigma x_1(1+x_1) \circ \mathrm{d}w_t, \\ \mathrm{d}x_2 &= [-\alpha x_1(1+x_1) - (1+x_1)^2 x_2]\mathrm{d}t - \sigma x_1(1+x_1) \circ \mathrm{d}w_t, \\ x_1(0) &= x_2(0) = 0.5, \end{aligned} \tag{27}$$

whose classical deterministic version has been used for modeling unforced periodic oscillations in certain chemical reactions.

This equation has been well-studied in the context of the theory of RDS in [26]. The deterministic Brusselator ($\sigma = 0$) has a fixed point $(x_1, x_2) = (0, 0)$, which is stable for $0 < a \leqslant 2$, unstable for $a > 2$ and and undergoes a Hopf bifurcation at the value $a = 2$. For the stochastic case ($\sigma \neq 0$), it was shown in [27] that the Lyapunov exponents remain negatives for the whole range of the parameter a and two different qualitative scenarios emerges. Namely, an asymptotically stable fixed point for $a < 2$ and a "limit cycle" for $a > 2$.

It is well-known that even in the deterministic case, many numerical methods fail to integrate Eq. (27) for $a > 2$ and moderate large step sizes. Fig. 4 shows the phase-portraits of this equation obtained by the Milstein,

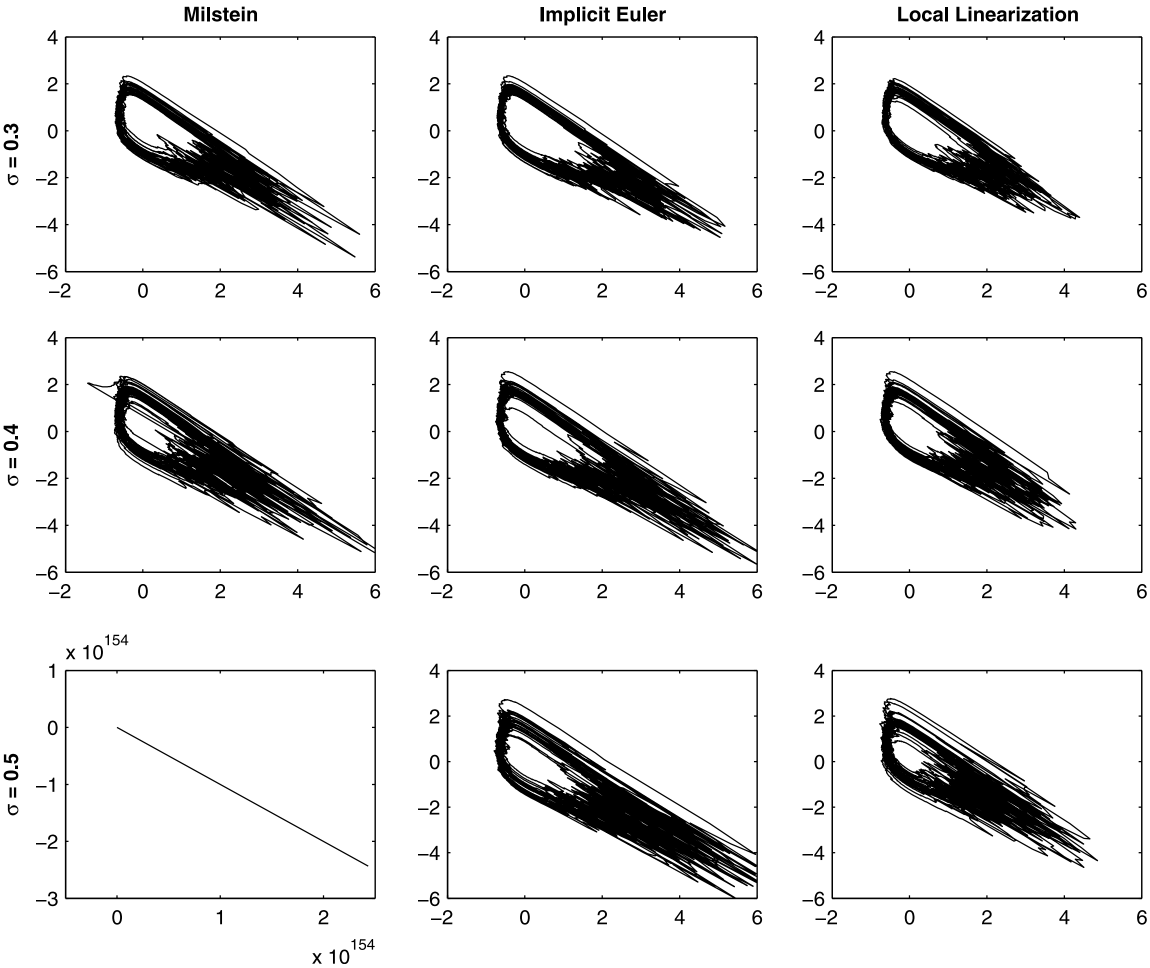

Fig. 4. Phase-portraits of Eq. (27) obtained by Milstein, implicit Euler and local linearization schemes for different values of the parameter σ, with $a = 3$ fixed. For each scheme, the plots show the approximations obtained with step-size $h = 2^{-5}$.

implicit Euler, and local linearization schemes for different values of the parameter σ, with $a = 3$ fixed. For each scheme, the plots show the approximations obtained over $0 \leqslant t \leqslant 200$ with step-size $h = 2^{-5}$. Notice that, for larger values of σ, the Milstein scheme lead to numerical explosions. On the contrary, the LL method shows more stable behavior for each value of the noise level σ.

The final example corresponds to the stochastic Duffing–van der Pol oscillator with both a multiplicative and an additive noise. This is described by the equation

$$\begin{aligned} dx_1 &= x_2\,dt, \\ dx_2 &= (-\alpha x_1 + \beta x_2 - x_1^2(x_1 + x_2))dt + \sigma_1 x_1 \circ dw_t^1 + \sigma_2 \circ dw_t^2, \\ x_1(0) &= x_2(0) = 1, \end{aligned} \tag{28}$$

where the parameters α, β are as in Eq. (26) and σ_1, σ_2 represent the intensities of the two independent noises. This equation was numerically integrated on the interval $0 \leqslant t \leqslant 50$ and the parameters were chosen as $\sigma_1 = 1$, $\beta = 1$, $\alpha = 1$ and $\sigma_2 = 8$. Fig. 5 shows the results obtained with the step-sizes $h = 2^{-3}, 2^{-4}, 2^{-7}$ by the LL scheme (25) and by the Milstein and implicit Euler as well. As in the previous figures, the LL method has a similar behavior to the implicit Euler scheme. Notice also that this result agrees with the ones reported by [1], which states the existence of a global attractor for the system (28).

The results of this section evidence that the LL scheme introduced in this paper achieves a convenient trade-off between numerical stability and computational cost, and reproduces the dynamics of SDEs much better

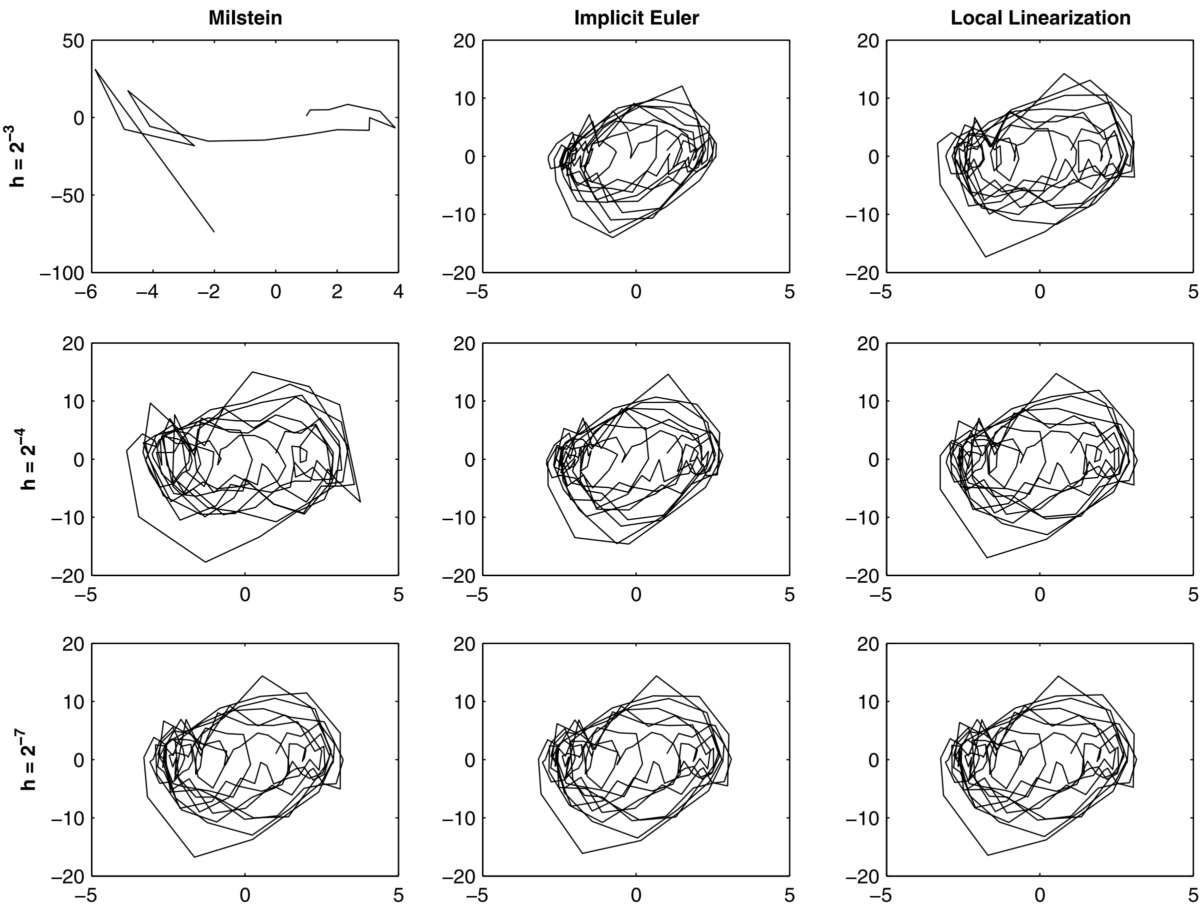

Fig. 5. Comparison of the Milstein, implicit Euler and local linearization scheme in the integration of Eq. (28) with values $\sigma_1 = 1$, $\sigma_2 = 8$, $\beta = 1$, $\alpha = 1$ corresponding to a limit cycle scenario. For each scheme, the phase-portraits show the approximations obtained with step-sizes $h = 2^{-3}, 2^{-4}, 2^{-7}$.

than standard explicit integrators. This agrees with similar results reported with LL schemes for ODEs, RDEs and SDEs with additive noise.

References

[1] P. Imkeller, B. Schmalfuss, The conjugacy of stochastic and random differential equations and the existence of global attractors, J. Dyn. Differen. Equat. 13 (2001) 215–249.
[2] P. Imkeller, C. Lederer, On the cohomology of flows of stochastic and random differential equations, Probab. Theory Relat. Fields 120 (2001) 209–235.
[3] P. Imkeller, C. Lederer, The cohomology of stochastic and random differential equations, and local linearization of stochastic flows, Stochast. Dyn. 2 (2002) 131–159.
[4] H. Doss, Liens entre 'equations diff' erentielles stochastiques et ordinaires, Ann. Inst. H. Poincaré Probab. Statist. XIII (1) (1977) 99–125.
[5] A.D. Ventzell, On the equation of the theory of conditional Markov processes, Theory Probab. Appl. 10 (1965) 357–361.
[6] D. Talay, Resolution trajectorielle et analyse numerique des equations differentielles stochastiques, Stochastics 9 (1983) 275–306.
[7] F. Castell, J. Gaines, The ordinary differential equation approach to asymptotically efficient schemes for solution of stochastic differential equations, Ann. Inst. Henri Poincaré 32 (2) (1996) 231–250.
[8] H. Schurz, Numerical analysis of stochastic differential equations without tears, in: D. Kannan, V. Lakshmikanthan (Eds.), Handbook of Stochastic Analysis and Applications, Marcel Dekker, Basel, 2002, pp. 237–359.
[9] H. de la Cruz, R.J. Biscay, F. Carbonell, J.C. Jimenez, T. Ozaki, Local Linearization-Runge Kutta (LLRK) methods for solving ordinary differential equations, Lecture Notes in Computer Sciences, vol. 3991, Springer-Verlag, 2006, pp. 132–139.
[10] H. de la Cruz, R.J. Biscay, F. Carbonell, T. Ozaki, J.C. Jimenez, A higher order local linearization method for solving ordinary differential equations, Appl. Math. Comput. 185 (2007) 197–212.
[11] F. Carbonell, J.C. Jimenez, R. Biscay, Cruz De la, The local linearization method for numerical integration of random differential equations, BIT Numer. Math. 45 (2005) 1–14.
[12] J.C. Jimenez, F. Carbonell, Local linear approximations for jump diffusion processes, J. Appl. Prob. 43 (2006) 185–194.
[13] M. Gitterman, The Noisy Oscillator, World Scientific, 2005.
[14] K. Bichteler, Stochastic integration with jumps, Encyclopedia of Mathematics and its Applications Series # 89, Cambridge University Press, 2002.
[15] A.T. Bharucha-Reid, Approximate Solution of Random Equations, North- Holland, New York and Oxford, 1979.
[16] L. Grune, P.E. Kloeden, Pathwise approximation of random ordinary differential equation, BIT 41 (2001) 711–721.
[17] C.F. Van Loan, Computing integrals involving the matrix exponential, IEEE Trans. Automat. Control 23 (1978) 395–404.
[18] R.B. Sidje, EXPOKIT: software package for computing matrix exponentials, AMC Trans. Math. Software 24 (1998) 130–156.
[19] C.B. Moler, C.F. Van Loan, Nineteen dubious methods for computing the matrix exponential, twenty-five years later, SIAM Rev. 45 (2003) 3–49.
[20] L. Dieci, A. Papini, Pade approximations for the exponential of a block triangular matrix, Linear Algebra Appl. 308 (2000) 103–202.
[21] J.C. Jimenez, A simple algebraic expression to evaluate the local linearization schemes for stochastic differential equations, Appl. Math. Lett. 15 (2002) 775–780.
[22] H. Keller, G. Ochs, Numerical approximation of random attractors, in: H. Crauel, M. Gundlach (Eds.), Stochastic Dynamics, Springer-Verlag, New York, 1999, pp. 93–115.
[23] K.R. Schenk-Hoppé, Bifurcation scenarios of the noisy Duffing–van der Pol oscillator, Nonlinear Dyn. 11 (3) (1996) 255–274.
[24] P. Imkeller, C. Lederer, Some formulas for Lyapunov exponents and rotation numbers in two dimensions and the stability of the harmonic oscillator and the inverted pendulum, Dyn. Syst.: Int. J. 16 (2001) 29–61.
[25] M. Ehrhardt, Invariant probabilities for systems in a random environment with applications to the Brusselator, Bull. Math. Biol. 45 (1983) 579–590.
[26] L. Arnold, G. Bleckert, K.R. Schenk-Hoppé, The stochastic Brusselator parametric noise destroys Hopf bifurcation, in: H. Crauel, M. Gundlach (Eds.), Stochastic Dynamics, Springer-Verlag, New York, 1999, pp. 71–92.
[27] L. Fronzoni, R. Mannella, P. McClintock, F. Moss, Postponement of Hopf bifurcation by multiplicative colored noise, Phys. Rev. A 36 (1987) 834–841.
[28] T. Shiga T, Mathematical results on the stepping stone model of population genetics, in: T. Ohta, K. Aoki (Eds.), Population Genetics and Molecular Evolution, Springer, 1985, pp. 267–279.
[29] L. Arnold, Random Dynamical Systems, Springer-Verlag, 1998.